

WAVEGUIDE MODELING OF LOSSY FLARED ACOUSTIC PIPES: DERIVATION OF A KELLY-LOCHBAUM STRUCTURE FOR REAL-TIME SIMULATIONS

Thomas Hélie, Rémi Mignot²

IRCAM & CNRS, UMR 9912,
1, place Igor Stravinsky, 75004 Paris, France
{helie, mignot}@ircam.fr

Denis Matignon

Télécom Paris/TSI & CNRS, UMR 5141
37-39, rue Dareau, 75014 Paris, France
denis.matignon@enst.fr

ABSTRACT

This paper deals with the theory and application of waveguide modeling of lossy flared acoustic pipes. The novelty lies in a refined 1D-acoustic model: the Webster-Lokshin equation. This model describes the propagation of longitudinal waves in axisymmetric acoustic pipes with a varying cross section, visco-thermal losses at the walls, and without assuming plane waves or spherical waves. Solving this model for a section of pipe leads to a quadrupole made of four transfer functions which imitate the global acoustic effects. Moreover, defining progressive waves and introducing some “relevant” physical interpretations enable the isolation of elementary transfer functions associated with elementary acoustic effects. From this decomposition, a standard Kelly-Lochbaum structure is recovered and efficient low-cost digital simulations are obtained. Thus, this work improves the realism of the sound synthesis of wind instruments, while it preserves waveguide techniques which only involve delay lines and digital filters.

1. INTRODUCTION

Because sound synthesis by physical models describes the acoustic mechanism of a musical instrument, it faithfully reproduces the behavior of the instrument, especially during attacks and note transitions, contrary to signal processing approaches. Moreover, parametric models allow makers to obtain new virtual instruments and explore new sounds, together with physical validation. However, digital time simulations require intensive computation from signal processors. That is why special care must be taken on the algorithmic complexity to perform real-time sound synthesis.

The aim of the present work is to build the whole resonator of a wind instrument by connecting several systems which imitate the acoustic of sections of pipes. To preserve the causality, the standard digital waveguide approach is used (see e.g. [2, 3]). The difficulty and the novelty is to include subtle, but perceptible, phenomena due to visco-thermal losses at the wall and continuously varying cross-sections (see e.g. [4, 5, 6]). The Webster-Lokshin equation is a 1D-acoustic model which describes the propagation of longitudinal waves in axisymmetric acoustic pipes involving such phenomena [5]. The following work therefore concentrates on recovering a standard Kelly-Lochbaum structure from this model and efficient low-cost digital simulations. The goal is to improve the realism of the sound synthesis of wind instruments using standard waveguide techniques.

¹ This work was carried out during a Masters degree program at University of Paris 6, see [1], and is supported by the CONSONNES project, ANR-05-BLAN-0097-01

² Ph.D. student at Telecom Paris / TSI

This paper is organized as follows. In section 2, the acoustic model, the acoustic state, and its decomposition into traveling waves are presented. The quadrupole describing a section of pipe is defined and the corresponding analytic transfer functions in the Laplace domain are given. Section 3 describes how a physical interpretation allows the isolation of some elementary acoustic phenomena, leading to a physically meaningful structure of the quadrupole. This structure is made of causal filters and a factorization isolates pure delays. In section 4, the concatenation of quadrupoles is performed and produces infinite instantaneous loops. This problem is removed using an algebraic computation, allowing for digital time simulation. The analysis of causality and stability are discussed. Section 5 presents the digital approximation of the transfer functions, the simulated structure, and the result of the real-time simulation in the time-domain. Then, this work is validated by comparing the impedance measured on a real instrument to that computed from the model. In section 6, we discuss the case of pipes with a varying cross-section characterized by a negative curvature, a case which involves unstable functions.

2. ACOUSTIC MODEL AND INPUT-OUTPUT REPRESENTATION OF A PIPE SECTION

2.1. Webster-Lokshin model

The Webster-Lokshin model is a mono-dimensional model which characterizes linear waves propagation in axisymmetric pipes, assuming only the quasi-sphericity of isobars near the inner wall (rather than plane waves or spherical waves), and taking into account visco-thermal losses [7, 5, 6]. The acoustic pressure p and the particle velocity v are governed by the following models, given in the Laplace domain:

$$\left(\left[\left(\frac{s}{c_0} \right)^2 + 2\varepsilon(l) \left(\frac{s}{c_0} \right)^{\frac{3}{2}} + \Upsilon(l) \right] - \partial_l^2 \right) r(l)p(l, s) = 0, \quad (1)$$

$$\rho_0 s v(l, s) + \partial_l p(l, s) = 0, \quad (2)$$

where s is the Laplace variable, $l \in [0, L]$ is the space variable measuring the arclength of the wall (but not the usual axis coordinate z , see [5]), $r(l)$ is the radius of the pipe, $\varepsilon(l) = \kappa_0 \sqrt{1 - r'(l)^2} / r(l)$ quantifies the visco-thermal losses ($\varepsilon(l) \geq 0$, because $|r'(l)| \leq 1$), and $\Upsilon(l) = r''(l) / r(l)$ accounts for the curvature of the pipe.

Note that the standard horn equation [8] corresponds to the nonlossy case $\varepsilon(l) = 0$ with a plane wave approximation so that the arclength l is approximated by the axis coordinate z . Bores and conical pipes are characterized by $\Upsilon(l) = 0$. If $\Upsilon(l)$ is negative, the transfer functions are unstable (see e.g.[9]). This problem is

discussed in section 6. In this paper, unless otherwise stated $\Upsilon(l)$ is assumed to be positive (straight, conical or flared pipes).

For standard conditions, the physical constants are the mass density $\rho_0 = 1.2 \text{ kg.m}^{-3}$, the speed of sound $c_0 = 344 \text{ m.s}^{-1}$ and the coefficient $\kappa_0 \approx 3.5 \cdot 10^{-4} \text{ m}^{-\frac{1}{2}}$.

2.2. Traveling waves

Let $\phi^+(l, t)$, $\phi^-(l, t)$ be defined by

$$\begin{bmatrix} \phi^+(l, s) \\ \phi^-(l, s) \end{bmatrix} = \frac{r(l)}{2} \begin{bmatrix} 1 & \rho_0 c_0 \\ 1 & -\rho_0 c_0 \end{bmatrix} \begin{bmatrix} p(l, s) \\ v(l, s) \end{bmatrix}. \quad (3)$$

For planar waves traveling inside a nonlossy bore, the acoustic state ϕ^\pm corresponds to the standard decoupled progressive planar waves. For the Wester-Lokshin model, these waves are still progressive so that they preserve the causality principle. They are governed by the following equations (see [7, p.59 & apdx. B1]):

$$\left[\frac{s}{c_0} \pm \partial_l \right] \phi^\pm(l, s) = \pm \zeta(l) \phi^\mp(l, s) - \varepsilon(l) \left(\frac{s}{c_0} \right)^{\frac{1}{2}} \phi(l, s), \quad (4)$$

where $\zeta(l) = r'(l)/r(l)$. The operator $[s/c_0 \pm \partial_l]$ is the traveling operator, and the right-hand side describes the coupling due to the curvature and the visco-thermal losses. Moreover, for bounded excitations, these progressive waves are also bounded, if $\varepsilon \geq 0$ (independently from the sign of Υ , see [10]).

2.3. Transfer matrix of the quadripole

Consider a section of pipe of length L with nearly constant curvature and losses $\Upsilon(l) = \Upsilon$ and $\varepsilon(l) = \varepsilon$, $\forall l \in [0, L]$. The acoustic model (1-2) can be solved analytically [7, p.63]. Then, from (3), the transfer matrix which characterizes the quadripole system with inputs $\phi^+(l=0, s)$, $\phi^-(l=L, s)$ and outputs $\phi^+(l=L, s)$, $\phi^-(l=0, s)$ (see fig. 1) can also be analytically derived [7, p.65]. It yields

$$\begin{bmatrix} \phi^+(L, s) \\ \phi^-(0, s) \end{bmatrix} = \begin{bmatrix} T(s) & R^l(s) \\ R^r(s) & T(s) \end{bmatrix} \begin{bmatrix} \phi^+(0, s) \\ \phi^-(L, s) \end{bmatrix}, \quad (5)$$

where the transmission T (independent from the direction), the

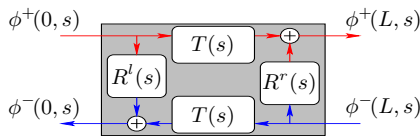


Figure 1: Representation of the quadripole.

left and right reflections, R^l and R^r respectively, are given by

$$T(s) = \left[A_T(s) \cosh(\Gamma(s)L) + B_T(s) \frac{\sinh(\Gamma(s)L)}{\Gamma(s)} \right]^{-1}, \quad (6)$$

$$R^l(s) = \left[A_R(s) \cosh(\Gamma(s)L) + B_{Rl}(s) \frac{\sinh(\Gamma(s)L)}{\Gamma(s)} \right] \frac{T(s)}{2}, \quad (7)$$

$$R^r(s) = \left[A_R(s) \cosh(\Gamma(s)L) + B_{Rr}(s) \frac{\sinh(\Gamma(s)L)}{\Gamma(s)} \right] \frac{T(s)}{2}, \quad (8)$$

where $\Gamma(s)$ is a square root of $\Gamma(s)^2 = \left(\frac{s}{c_0}\right)^2 + 2\varepsilon\left(\frac{s}{c_0}\right)^{\frac{3}{2}} + \Upsilon$, and A_T , B_T , A_R , B_{Rl} , and B_{Rr} are simple functions of: s , ζ_0 , ζ_L , $\Gamma(s)^2$ and c_0 .

3. DECOMPOSITION INTO FILTERS AND DELAYS

3.1. Acoustic interpretation of the progressive waves

The transfer functions R^r , R^l , and T represent the global effect of the whole section of pipe on the progressive waves ϕ^\pm . Nevertheless, some elementary effects can be isolated using the following physical interpretations (see Fig.2):

At the left extremity ($l=0$), the incident wave ϕ_0^+ is partially reflected in the opposite direction (modeled in Fig.2 by the transfer function R_{le}) and is partially transmitted into the pipe section (T_{le}). Then, this *transmitted part* travels inside the pipe until the right extremity located at $l=L$ (T_p^+), before being partially reflected (R_{ri}) and partially transmitted (T_{ri}) outside the pipe. Symmetrically, the incident wave ϕ_L^- undergoes similar phenomena.

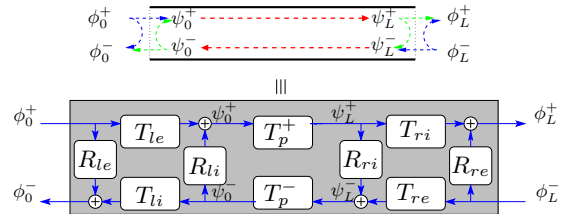


Figure 2: Physical interpretation and its representation with filters

The figure 2 compiles these phenomena and includes all the contributions (the indexes i and e mean respectively *internal* and *external*; the functions T_p^+ and T_p^- symbolize respectively the forward and the backward propagation transmission through the pipe).

The quadripoles described in figures 1 and 2 are equivalent if the following algebraic equations holds:

$$T = T^+ = \frac{T_{le} T_{ri} T_p^+}{1 - R_{ri} R_{li} T_p^- T_p^+} \quad (9)$$

$$= T^- = \frac{T_{re} T_{li} T_p^-}{1 - R_{ri} R_{li} T_p^- T_p^+}, \quad (10)$$

$$R^l = R_{le} + \frac{R_{ri} T_{le} T_{li} T_p^+ T_p^-}{1 - R_{ri} R_{li} T_p^- T_p^+}, \quad (11)$$

$$R^r = R_{re} + \frac{R_{li} T_{re} T_{ri} T_p^+ T_p^-}{1 - R_{ri} R_{li} T_p^- T_p^+}. \quad (12)$$

These equations do not lead to a unique identification of (T_{li} , R_{li} , T_{le} , R_{le} , T_p^+ , T_p^- , T_{ri} , R_{ri} , T_{re} , R_{re}) from (6-8). Nevertheless, additional meaningful assumptions cope with this problem.

3.2. Identification of the transfer functions

Assuming the following hypotheses yields a unique identification:

(H1) The pressure continuity $\phi_l^+ + \phi_l^- = \psi_l^+ + \psi_l^-$ for $l \in \{0, L\}$ is required (see Fig. 2), so that *every reflection r and every transmission t fed by the same input are such that $t = 1 + r$* .

(H2) The left-hand side functions depend only on the *left parameter* ζ_0 . Respectively, the right-hand side functions depend only on the *right parameter* ζ_L .

(H3) The propagation transfer functions T_p^\pm include a pure delay operator: $T_p^\pm(s) = \tilde{T}_p^\pm(s) e^{-sL/c_0}$, where $\tilde{T}_p^\pm(s) = e^{-(\Gamma(s)-s/c_0)L}$ stays causal and stable, see section 4.3.

In this case, the unique solution is:

$$T_p^+(s) = T_p^-(s) = T_p(s) = e^{-\Gamma(s)L}, \quad (13)$$

$$R_{re}(s) = -\frac{\Gamma(s) - \frac{s}{c_0} - \zeta_L}{\Gamma(s) + \frac{s}{c_0} - \zeta_L} = 1 - T_{re}(s), \quad (14)$$

$$R_{le}(s) = -\frac{\Gamma(s) - \frac{s}{c_0} + \zeta_0}{\Gamma(s) + \frac{s}{c_0} + \zeta_0} = 1 - T_{le}(s), \quad (15)$$

$$R_{ri}(s) = \frac{\Gamma(s) - \frac{s}{c_0} + \zeta_L}{\Gamma(s) + \frac{s}{c_0} - \zeta_L} = 1 - T_{ri}(s), \quad (16)$$

$$R_{li}(s) = \frac{\Gamma(s) - \frac{s}{c_0} - \zeta_0}{\Gamma(s) + \frac{s}{c_0} + \zeta_0} = 1 - T_{li}(s). \quad (17)$$

Note that, contrary to (6-8), these functions are not functions of $\Gamma(s)^2$. In the following, we choose to define $\Gamma(s)$ for $s \in \mathbb{C}_0^+ = \{s \in \mathbb{C} \mid \Re(s) > 0\}$, as the unique analytic continuation of the positive square root of $\Gamma(s)^2$ for $s \in \mathbb{R}^+$. The analyticity for $\Re(s) > 0$ holds because $\Gamma(s)$ has no branching points in \mathbb{C}_0^+ , if $\Upsilon \geq 0$. This defines causal stable systems (see [6] for details).

4. BUILDING A WHOLE RESONATOR

4.1. Concatenating quadripoles

The whole resonator of a wind instrument with radius $r^*(l)$ is first approximated by the concatenation of K sections of pipes with constant parameters ϵ_k, Υ_k and length L_k ($1 \leq k \leq K$), such that the approximated radius $r(l)$ is \mathcal{C}^1 -regular. This implies that $\zeta = r'/r$ is continuous with respect to l , that is, $\zeta_r^{(k)} = \zeta_l^{(k+1)}$.

Assuming the continuity of the pressure and the flow, the virtual resonator is built by successively connecting the quadripoles \mathbf{Q}_k (see Fig.3), associated to the corresponding sections of pipe.

4.2. Removing infinite instantaneous loops

Connecting two quadripoles creates an instantaneous loop which cannot be simulated digitally (see Fig.3, top). This difficulty is overcome using algebraic calculations (see [6]) which lead to the structure presented in Fig.3 (bottom), where a reflection function

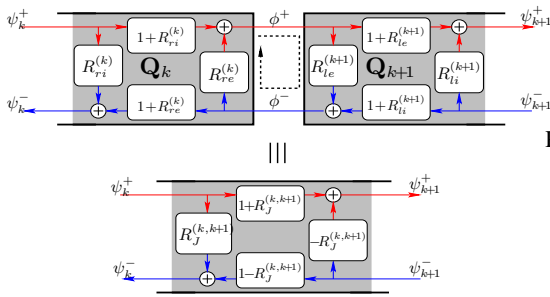


Figure 3: Connecting quadripoles and removing instantaneous loops

of the junction $R_J^{(k,k+1)}$ is introduced and given by:

$$R_J^{(k,k+1)}(s) = \frac{\Gamma_{k+1}(s) - \Gamma_k(s)}{\Gamma_{k+1}(s) + \Gamma_k(s)}, \quad (18)$$

and where Γ_k is the function Γ with the losses and the curvature coefficients of the quadripole k , characterized by a length L_k and coefficients ϵ_k, Υ_k .

4.3. Stability and causality analysis

It is proven in [1] that for all section k such that $\Upsilon_k \geq 0$, the function $\Gamma_k(s)$ satisfies $\Re(\Gamma_k(s)) > 0$ and $\text{sign}(\Im(\Gamma_k(s))) = \text{sign}(\Im(s))$, for all $s \in \mathbb{C}_0^+$. From this, it can be deduced that the functions $R_J^{(k,k+1)}$ and T_p^k are such that $|R_J^{(k,k+1)}(s)| < 1$ and $|T_p^k(s)| < 1$, for all $s \in \mathbb{C}_0^+$ and that they both define stable systems. Moreover, their asymptotic expansions for $|s| \rightarrow +\infty$ with $s \in \mathbb{C}_0^+$ make it possible to prove the causality of the associated systems (see [6, 1]).

Finally, the whole system (including all the quadripoles) is proven to be causal. Nevertheless, its global stability must still be proven (from the previous inequalities). This will be the object of a future, in-depth study. At present, all numerical simulations have satisfied this property.

5. APPROXIMATION AND DIGITAL SIMULATION

5.1. Diffusive representation and approximation

If $\Upsilon = 0$, the function Γ has one branching point $s = 0$. We choose the cut as \mathbb{R}^- to preserve the hermitian symmetry. Thereof, every transfer function has a continuous line of singularities on \mathbb{R}^- . The residues theorem shows that these functions are represented by a class of infinite-dimensional system, called *Diffusive Representations* [11]. For any diffusive representation $H(s)$ which is analytic on $\mathbb{C} \setminus \mathbb{R}^-$:

$$H(s) = \int_0^\infty \frac{\mu_H(\xi)}{s + \xi} d\xi, \quad (19)$$

$$\mu_H(\xi) = \frac{1}{2i\pi} \{H(-\xi + i0^-) - H(-\xi + i0^+)\}. \quad (20)$$

In [12], it is proposed to approximate such diffusive representations by finite-dimensional approximations, given by $\tilde{H}_\mu(s) = \sum_{j=1}^J \frac{\mu_j}{s + \xi_j}$, where J is the number of poles, $-\xi_j \in \mathbb{R}^-$ is the position of the pole number j and μ_j is its weight. The poles are placed in \mathbb{R}^- with a logarithmic scale, and the weights μ_j are obtained by a least-square optimization in the Fourier domain.

If $\Upsilon > 0$, Γ has two more branching points, which are complex conjugate. In this case, the diffusive representations are approximated with a finite sum of first and second order differential systems. Finally, a digital version is implemented using standard numerical approximations (see [6]).

5.2. Real-time simulation

According to [13], the quadripole in figure 3 (bottom) can be rewritten as in figure 4. This structure allows a significant reduction of the number of filters implemented and so decreases the processor use for the real-time simulation.

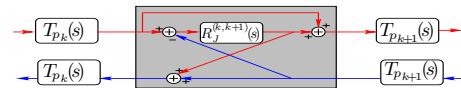


Figure 4: Simulated structure of the junction quadripole

The figure 5 shows the impulse responses of a virtual instrument made of a mouth-piece³, a bore, a bell with constant curvature, and a radiation impedance [15]. P_{mp}^- is the backward pressure from the mouth-piece, and P_r is the radiated pressure.

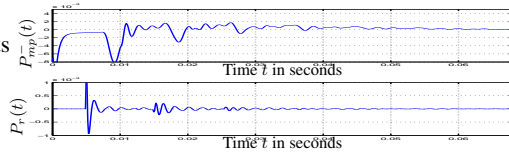


Figure 5: Impulse responses of the resonator

The figure 6 shows the comparison of the input impedance measured on a real trombone⁴ with the input impedance computed from the model (with or without losses) for a resonator described by five sections of pipe. The parameters of the pipe sections have been tuned from the geometrical shape measured on the real instrument. The computed impedance fits with measurements if re-

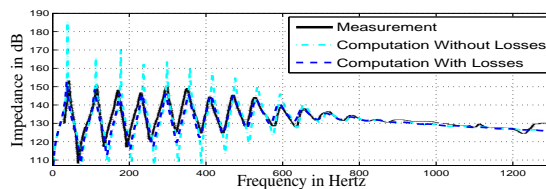


Figure 6: Measured and computed impedances with/without losses

alistic losses are included ($\varepsilon > 0$). Otherwise ($\varepsilon = 0$), the quality factor of the resonances are significantly overestimated. Furthermore, using cones rather than flared pipes would shift the frequencies of the resonances, unless the number of sections of pipe are increased. This highlights the accuracy of the Webster-Lokshin model compared to more simplified and approximated models: in terms of sound quality, using five cones would detune the instrument and discarding losses would lead to more metallic and synthetic sounds.

A real-time version of this has been implemented in C-language (plug-in for Pure Data).

6. CONCLUSIONS AND PERSPECTIVES

In this paper, an efficient real-time simulation of flared acoustic pipes using a Kelly-Lochbaum structure and digital waveguides has been proposed for a Webster-Lokshin acoustic model. Comparisons between numerical results and experimental measures on a trombone prove to be accurate.

For negative curvatures Υ , the stability of the quadripole in fig.1 is preserved, but the elementary transfer functions (13-17) are unstable. As a consequence, the Kelly-Lochbaum structure in Fig.4 is useless in this case. This problem is well-known [16, 9] and understood [17]: the elementary functions govern the waves propagation in pipes with infinite length; they are unstable if the pipe is convergent. Nevertheless, as the global quadripole proves

³The mouth-piece is modeled by an acoustic mass, resistance and compliance in the low frequency approximation, see [14]

⁴These data correspond to a *Courtois* trombone. The authors thank René Caussé for having given these data.

to be stable, stable decompositions is not hopeless: further works will be carried out to cope with this problem.

Acknowledgment

The authors thank Deborah Lopatin for proofreading this paper.

7. REFERENCES

- [1] R. Mignot, "Modélisation de résonateurs d'instruments à vent," Master M2 ATIAM, Université Paris 6, Paris, 2006.
- [2] J. O. Smith, "Physical modeling synthesis update," *Computer Music Journal*, vol. 20, no. 2, pp. 44–56, 1996, MIT Press.
- [3] V. Välimäki, "Discrete-time modeling of acoustic tubes using fractional delay filters," Ph.D. dissertation, Helsinki University of Technology, 1995.
- [4] J.-D. Polack, "Time domain solution of Kirchhoff's equation for sound propagation in viscothermal gases: a diffusion process," *J. Acoustique*, vol. 4, pp. 47–67, Feb. 1991.
- [5] T. Hélie, "Unidimensional models of acoustic propagation in axisymmetric waveguides," *J. Acoust. Soc. Am.*, vol. 114, pp. 2633–2647, 2003.
- [6] T. Hélie and D. Matignon, "Diffusive representations for the analysis and simulation of flared acoustic pipes with viscothermal losses," *Mathematical Models and Methods in Applied Sciences*, vol. 16, pp. 503–536, jan 2006.
- [7] T. Hélie, "Modélisation physique des instruments de musique en systèmes dynamiques et inversion," Ph.D. dissertation, Université Paris-Sud, Orsay, France, 2002.
- [8] A. Webster, "Acoustic impedance and the theory of horns and of the phonograph," *Proc. Nat. Acad. Sci. U.S.*, vol. 5, 1919.
- [9] E. Ducasse, "An alternative to the traveling-wave approach for use in two-port descriptions of acoustic bores," *J. Acoust. Soc. Am.*, vol. 112, pp. 3031–3041, 2002.
- [10] T. Hélie, "Ondes découplées et ondes progressives pour les problèmes mono-dimensionnels d'acoustique linéaire," in *CFA*, Tours, France, 2006.
- [11] G. Montseny, "Diffusive representation of pseudo-differential time-operators," *ESAIM*, vol. 5, pp. 159–175, 1998.
- [12] T. Hélie, D. Matignon, and R. Mignot, "Criterion design for optimizing low-cost approximations of infinite-dimensional systems: Towards efficient real-time simulation," *Int. Journal of Tomography and Statistics*, pp. 13–18, 2007.
- [13] J. D. Markel and A. H. Gray, "On autocorrelation equations as applied to speech analysis," *IEEE Trans. Audio and Electroacoust.*, vol. AU-21, no. 2, pp. pp. 69–79, Apr 1973.
- [14] N. H. Fletcher and T. D. Rossing, *Physics of musical instruments*. New York: Springer Verlag, 1991.
- [15] T. Hélie and X. Rodet, "Radiation of a pulsating portion of a sphere: application to horn radiation," *Acta Acustica*, vol. 89, pp. 565–577, 2003.
- [16] D. Berners, "Acoustics and signal processing techniques for physical modeling of brass instruments," Ph.D. dissertation, Stanford University, 1999.
- [17] J. Gilbert, J. Kergomard, and J. D. Polack, "On the reflection functions associated with discontinuities in conical bores," *J. Acoust. Soc. Am.*, vol. 04, 1990.